JOURNAL OF GUIDANCE, CONTROL, AND DYNAMICS
Vol. 38, No. 6, June 2015

Impulsive Maneuvers for Formation Reconfiguration Using Relative Orbital Elements

G. Gaias* and S. D'Amico†
DLR, German Aerospace Center, 82234 Wessling, Germany

DOI: 10.2514/1.G000189

Advanced multisatellite missions based on formation-flying and on-orbit servicing concepts require the capability to arbitrarily reconfigure the relative motion in an autonomous, fuel efficient, and flexible manner. Realistic flight scenarios impose maneuvering time constraints driven by the satellite bus, by the payload, or by collision avoidance needs. In addition, mission control center planning and operations tasks demand determinism and predictability of the propulsion system activities. Based on these considerations and on the experience gained from the most recent autonomous formation-flying demonstrations in near-circular orbit, this paper addresses and reviews multi-impulsive solution schemes for formation reconfiguration in the relative orbit elements space. In contrast to the available literature, which focuses on case-by-case or problem-specific solutions, this work seeks the systematic search and characterization of impulsive maneuvers of operational relevance. The inversion of the equations of relative motion parameterized using relative orbital elements enables the straightforward computation of analytical or numerical solutions and provides direct insight into the delta-v cost and the most convenient maneuver locations. The resulting general methodology is not only able to refind and requalify all particular solutions known in literature or flown in space, but enables the identification of novel fuel-efficient maneuvering schemes for future onboard implementation.

Nomenclature

a	=	semimajor axis
$\mathbf{B}$	=	control input matrix of the relative dynamics model
e	=	eccentricity
i	=	inclination
n	=	mean angular motion
u	=	mean argument of latitude
$\Delta\bullet$	=	finite variation of a quantity
$\delta\boldsymbol{e}$	=	nondimensional relative eccentricity vector
$\delta\boldsymbol{i}$	=	nondimensional relative inclination vector
$\delta\boldsymbol{\alpha}$	=	nondimensional relative orbital elements relative orbital elements set
$\delta\lambda$	=	nondimensional relative longitude
δv_R, δv_T, δv_N	=	instantaneous velocity changes in local radial, tangential and normal directions
$\delta\bullet$	=	relative quantity
θ	=	argument of latitude of the relative ascending node
$\mathbf{\Phi}$	=	state transition matrix of the relative dynamics model
φ	=	argument of latitude of the relative perigee
Ω	=	right ascension of the ascending node
ω	=	argument of perigee

I. Introduction

THE capability to establish, reconfigure, and maintain suitable relative motions between coorbiting vehicles represents a key requirement for spacecraft formation-flying and on-orbit servicing missions. Realistic operational scenarios ask for accomplishing such actions in a safe way, within certain levels of accuracy, and in a fuel-efficient manner. Moreover, distributed space systems might be subject to maneuvering time constraints dictated by the satellite bus and payload needs. In this context, this work addresses simple and practical impulsive reconfiguration schemes useful to maneuver planners for autonomous onboard applications. Focus is given to the comparison of the delta-v expenditure and to the understanding of the shape of the relative motion that is obtained during the transition phases. This last point is crucial in the assessment of the formation safety [1].

So far, various models of the linearized relative motion have been presented in the literature. They differ in the choice of the coordinates, in the range of applicability (e.g., eccentricity of the chief orbit, separation as compared with orbit radius), and in the disturbances they include. According to the choice of the variables' set, the proposed models could be roughly grouped in the following families: models based on the Cartesian relative state [2–5], models that make use of geometrical quantities defined from the analytical solution of the Hill–Clohessy–Wiltshire equations (HCW) [6,7], models based on the difference of absolute orbital elements [8–10], and models that exploit the relative orbital elements (ROEs) as inherited from the colocation of geostationary satellites [1,11–14]. In addition to these commonly used parameterizations, some more abstract options are available. In particular, differences of absolute Eulerian elements allow including perturbations till part of the fourth zonal harmonic of the Earth's gravity potential [15]. Kasdin et al. set up a Hamiltonian approach to derive canonical coordinates for the relative state-space dynamics in a circular reference orbit [16]. A description of the relative motion using quaternions is provided in [17].

The problem of establishing and maintaining a formation has also been widely addressed. Proposed methodologies range from continuous to impulsive control techniques. The former approaches are mainly suited for forced motion phases and/or when low-thrust actuation systems are employed. Impulsive control is generally preferred to cope with payload constraints because instruments might be disturbed by the orbit correction maneuvers. Moreover impulsive closed-form schemes can be advantageous, both in terms of mission operations and mission planning. Impulsive control has been extensively used during various phases of the Prototype Research Instruments and Space Mission Technology Advancement (PRISMA) mission [18] and is foreseen for the far- to midrange approach phases of the Deutsche Orbitale Servicing (DEOS) mission [19].

Received 30 July 2013; revision received 19 December 2013; accepted for publication 20 December 2013; published online 25 April 2014.

*Research Engineer, German Space Operations Center/Space Flight Technology, Münchner Str. 20; gabriella.gaias@dlr.de.

†German Space Operations Center/Space Flight Technology; currently Assistant Professor, Stanford University, Department of Aeronautics and Astronautics, Durand Building, Stanford, CA 94305; damicos@stanford.edu.

Tillerson et al. proposed fuel-optimal guidance and control strategies based on convex optimization techniques [20,21]. The linear time-varying equations of the linearized relative motion in the Cartesian relative state are discretized and a linear programming problem is set up to minimize the weighted sum of the norm-1 of the control inputs. Terminal conditions (for the guidance phase) or state-space constraints (for the control phase) are introduced as inequality convex constraints [20,21]. The time discretization required to describe the fast varying dynamics, especially for eccentric reference orbits, can lead to prohibitive computational loads for spaceborne microprocessors. Larsson et al. carried on with this approach, though employing the Yamanaka–Ankersen state transition matrix [5] to allow larger time steps, but neglecting the mean effects of J_2 in the model of the dynamics [22]. Such algorithm was implemented onboard within the PRISMA mission and successfully demonstrated in-flight [18]. A further limitation of this strategy is related to the management of maneuvers' exclusion windows and to the predictability of control correction maneuvers, both key issues in certain typologies of scientific missions (e.g., TanDEM-X [23]).

Classical impulsive control techniques are often based on the exploitation of the Gauss variational equations (GVE). In the case when the relative motion is parameterized through differences of mean absolute elements, Vadali et al. proposed a method to initialize the relative motion [24], whereas Schaub and Alfriend presented an impulsive feedback controller [25]. An analytical solution for the optimal reconfiguration problem was proposed by Vaddi et al. [26]. It accomplishes the in-plane correction through a couple of impulses in the radial direction of the local orbital frame. Ichimura and Ichikawa made use of a parameterization defined from the analytical solution of the HCW equations to develop an analytical open-time minimum-fuel reconfiguration strategy [7]. It involves three in-plane impulses to achieve optimal reconfigurations in the case that the aimed change in the size of the formation is greater than the change in the drift and enough transfer time is available. Starting from this open-loop profile, they designed a suboptimal feedback controller. Jifuku et al. extended this approach by considering that impulsive maneuvers take place over a finite, limited, and fixed pulses time [27]. Finally, the recent flight demonstrations, namely, the Spaceborne Autonomous Formation Flying Experiment (SAFE) [28] and the TanDEM-X Autonomous Formation Flying (TAFF) system [29], make use of practical and simple closed-form solutions of the GVE, which result from the inversion of the model of the relative dynamics expressed in terms of ROEs [13]. In particular, TAFF accomplishes pairs of (anti-) along-track maneuvers separated by half an orbital revolution for in-plane formation keeping only, whereas SAFE can also exploit radial and cross-track pulses for enhanced in-plane and out-of-plane control, respectively. Both systems realize an autonomous formation control, where maneuvers are planned and executed onboard, to acquire nominal or desired formation configurations (i.e., guidance) prescribed from ground through telecommands.

This work addresses the formation reconfiguration problem over limited and defined time spans: a reconfiguration is seen as the achievement of a certain user-defined set of ROEs at the final time of the reconfiguration horizon. The relative dynamics is parameterized through ROEs to exploit their direct insight of the geometry of the relative motion and the existence of simple relations between changes in ROE and applied delta-v.

Therefore, thanks to both problem setting and choice of the parameterization, this work defines a general framework in which to explore and compare different reconfiguration strategies involving a limited number of impulsive maneuvers. In contrast with the available literature, which focuses on case-by-case or problem-specific solutions, this work provides different maneuvering schemes that are able to satisfy the complete set of end conditions at the final time. The available methodologies are then classified according to the application scenarios with which they can deal. As a result, it is possible to recognize some previously published methodologies and, on the one hand, to discuss their range of applicability, and, on the other hand, to generalize such solutions.

Besides the application scenarios, this work also investigates other characteristics of the feasible reconfiguration strategies, relevant for realistic onboard applications: the easiness of computation of the required maneuvers and how the intermediate ROEs move in the ROE space. This topic is considered because several features (e.g., delta-v minimization, passive safety, satisfaction of visibility constraints) are easily referable to well-defined configurations in the ROE space.

A further contribution of this work is the systematic comparison of the delta-v costs achievable by all the feasible maneuvering schemes with respect to the absolute minimum reconfiguration cost. To this end, the in-plane delta-v lower bound presented in [7,30] has been generalized to take into account when large changes of mean relative longitude occur over finite reconfiguration horizons. Moreover, by depicting each feasible reconfiguration strategy in the ROE space, this work discusses the geometrical interpretation of the sources that contributed to gain the delta-v cost. Consequently, the in-plane maneuver locations to fulfill the delta-v minimization are straightforwardly derived from these geometrical considerations, in agreement with [14,30].

The ultimate scope of this work is to support the decision process of a maneuver planner that, among several feasible solution schemes, has to select a preferred one based on some planning drivers, such as thrusters' duty cycle, attitude constraints, passive safety, visibility constraints, maneuvers' determinism and predictability, and delta-v minimization.

The paper is organized as follows. First, the theory of ROEs is shortly recalled and the reconfiguration framework is defined. Second, a lower bound for the in-plane delta-v cost is introduced and its meaning in terms of ROEs is analyzed. Subsequently, a systematic search and analysis of two and three impulses solution schemes are carried out. It is emphasized that only the options able to satisfy the complete set of final ROEs at the final time are addressed in this paper. These solutions differ in their structure, because some assumptions are introduced to either reduce the size of the solutions' space or to ease their computation toward an analytical form. Despite the fact that these assumptions might be suggested by a physical interpretation of the problem, they introduce constraints that impact the characteristics of such solutions. Before concluding, this work provides some guidelines to support the design of a maneuver planner, suitable also for onboard applications. The provided instructions are based on the general methodology developed across the paper and wrap up when to exploit the available (i.e., requalified and newly developed) solution schemes.

II. Relative Motion Equations

The relative motion is described by this set of dimensionless ROEs:

$$\delta\boldsymbol{\alpha} = \begin{pmatrix} \delta a \\ \delta\lambda \\ \delta e_x \\ \delta e_y \\ \delta i_x \\ \delta i_y \end{pmatrix} = \begin{pmatrix} \delta a \\ \delta\lambda \\ \delta e \cos\varphi \\ \delta e \sin\varphi \\ \delta i \cos\theta \\ \delta i \sin\theta \end{pmatrix} = \begin{pmatrix} (a - a_d)/a_d \\ u - u_d + (\Omega - \Omega_d)\cos i_d \\ e\cos\omega - e_d\cos\omega_d \\ e\sin\omega - e_d\sin\omega_d \\ i - i_d \\ (\Omega - \Omega_d)\sin i_d \end{pmatrix} \tag{1}$$

where a, e, i, ω, Ω, and M denote the classical Keplerian elements and $u = M + \omega$ is the mean argument of latitude. The subscript d denotes quantities referring to the deputy spacecraft, which defines the origin of the local radial (R) –tangential (T) –normal (N) frame. The quantities δa, $\delta\lambda = \delta u + \delta i_y \cot i$, $\delta\boldsymbol{e}$, and $\delta\boldsymbol{i}$ represent the relative semimajor axis, the relative mean longitude, and the relative eccentricity and inclination vectors, respectively. D'Amico [13,14] provides assumptions and descriptions of the model. According to it, the relative mean longitude changes as a function of the mean argument of latitude and of δa according to

$$\delta\lambda(u) = -1.5(u - u_0)\delta a + \delta\lambda(u_0) = -1.5(u - u_0)\delta a + \delta\lambda_0 \tag{2}$$

and an impulsive maneuver at the mean argument of latitude u_M produces these ROE variations:

$$
\begin{aligned}
a\Delta\delta a &= +2\delta v_T/n, \qquad a\Delta\delta i_x = +\delta v_N \cos u_M/n \\
a\Delta\delta\lambda &= -2\delta v_R/n, \qquad a\Delta\delta i_y = +\delta v_N \sin u_M/n \\
a\Delta\delta e_x &= +\delta v_R \sin u_M/n + 2\delta v_T \cos u_M/n \\
a\Delta\delta e_y &= -\delta v_R \cos u_M/n + 2\delta v_T \sin u_M/n
\end{aligned} \tag{3}
$$

Here the dimensional jump is considered and the subscript d is dropped.

By considering Eq. (3) and the model of the relative dynamics, the following features will be exploited in the remainder of the paper to deal with the maneuvers' planning problem:

1) In-plane and out-of-plane motions are decoupled thanks to the choice of employing $\delta\lambda$ instead of δu in the variables' set. In this case, in fact, the variation of mean argument of latitude generated by a thrust in cross-track direction is balanced by the equal and opposite term contained in the definition of the relative longitude ([14] p. 42).

2) There are two possible ways for achieving a variation of $\delta\lambda$: either instantaneously with a radial delta-v or within some time, making use of the natural dynamics of the system, by establishing a given δa through a tangential delta-v.

3) There is an intrinsic relationship between the drift component δa and the relative eccentricity vector $\delta\boldsymbol{e}$ and it is convenient to exploit such a synergy by maneuvering at those mean arguments of latitude that are convenient for achieving an aimed variation of relative eccentricity vector, being drift corrections independent from the location of the maneuver.

4) A certain change in the magnitude of the relative eccentricity vector can be achieved either by maneuvers perfectly aligned with the radial or with the tangential direction. In the first case, the required magnitude of delta-v is double as shown in Eq. (3).

5) Tangential delta-v allows changing all the elements of the in-plane subset, either instantaneously or within some time. When only tangential maneuvers are performed, a given magnitude of the applied delta-v generates the same change in the magnitude of δa and $\|\delta\boldsymbol{e}\|$, thus distances in the ROE space constitute a metric of the reconfiguration cost.

According to our framework, a reconfiguration from a certain initial relative orbit to an aimed final one can be defined as the transition $\delta\boldsymbol{\alpha}_0 \to \delta\boldsymbol{\alpha}_F$ over the finite time interval to span $[u_0, u_F]$. The explicit involvement of the final time does not reduce the generality of the treatment but allows addressing more practical scenarios in which a reconfiguration has to cope with possible requirements coming from the space segment. Moreover, if we consider the typical scenario of a reconfiguration between two bounded relative orbits (i.e., $\delta a_0 = \delta a_F = 0$), the limited reconfiguration horizon assumes the meaning of maximum allowed transfer time. In this case, in fact, $\delta\lambda$ is also constant and whatever mean argument of latitude of the starting and final relative orbits becomes a candidate for locating the first and last maneuvers, respectively.

The following notations are introduced:

$$
\begin{aligned}
\delta\boldsymbol{\alpha}(u_1) &= \boldsymbol{\Phi}(u_1, u_0)\delta\boldsymbol{\alpha}(u_0) = \Phi_{1,0}\delta\boldsymbol{\alpha}_0, \\
\Delta\delta\boldsymbol{\alpha}(u_j) &= \frac{1}{v}\mathbf{B}(u_j)\delta\mathbf{v} = \frac{1}{v}\mathbf{B}_j\delta\mathbf{v}
\end{aligned} \tag{4}
$$

where $v = na$, the state transition matrix $\boldsymbol{\Phi}$ describes the natural dynamics over the interval $[u_0, u_1]$, and the control input matrix $\mathbf{B}$ expresses the effects of the maneuvers performed at the mean arguments of latitude u_j. Therefore, the reconfiguration $\delta\boldsymbol{\alpha}_0 \to \delta\boldsymbol{\alpha}_F$ can be written as

$$
\begin{aligned}
&(\boldsymbol{\Phi}_{F,1}\mathbf{B}_1 \quad \cdots \quad \boldsymbol{\Phi}_{F,p}\mathbf{B}_p)\delta\mathbf{v} = na(\delta\boldsymbol{\alpha}_F - \boldsymbol{\Phi}_{F,0}\delta\boldsymbol{\alpha}_0) \\
&\mathbf{M}\delta\mathbf{v} = n\Delta\delta\tilde{\boldsymbol{\alpha}}
\end{aligned} \tag{5}
$$

where p maneuvers are performed to meet all the state end conditions $\Delta\delta\tilde{\boldsymbol{\alpha}}$ at u_F, according to

$$
\begin{aligned}
\delta\boldsymbol{\alpha}_1 &= \boldsymbol{\Phi}_{1,0}\delta\boldsymbol{\alpha}_0 + \frac{1}{v}\mathbf{B}_1\delta\mathbf{v}_1 \\
\delta\boldsymbol{\alpha}_2 &= \boldsymbol{\Phi}_{2,1}\delta\boldsymbol{\alpha}_1 + \frac{1}{v}\mathbf{B}_2\delta\mathbf{v}_2 = \boldsymbol{\Phi}_{2,0}\delta\boldsymbol{\alpha}_0 + \frac{1}{v}\boldsymbol{\Phi}_{2,1}\mathbf{B}_1\delta\mathbf{v}_1 + \frac{1}{v}\mathbf{B}_2\delta\mathbf{v}_2 \\
&\vdots \\
\delta\boldsymbol{\alpha}_F &= \boldsymbol{\Phi}_{F,p}\delta\boldsymbol{\alpha}_p + \frac{1}{v}\mathbf{B}_p\delta\mathbf{v}_p
\end{aligned} \tag{6}
$$

In this work, we are focusing on maneuvering schemes to accomplish a single reconfiguration on a limited time span, thus $\boldsymbol{\Phi}$ is the state transition matrix of the Keplerian relative motion. Nevertheless, the establishment of a certain relative motion could be considered part of a larger guidance plan, based on the evolution of Eq. (6) as accomplished in [31]. Consequently, the state transition matrix of the linearized relative motion $\boldsymbol{\Phi}$ is modified to include the mean effects due to the J_2 Earth oblateness and the linear in time variation of the relative semimajor axis due to the action of the differential drag. These contributions determine a global correction of the effective jump to be realized [i.e., $\Delta\delta\tilde{\boldsymbol{\alpha}}$ of Eq. (5)].

Being the state variable composed of two independent subsets, Eq. (5) represents the contemporaneous solution of two disjointed problems, namely, the in-plane and out-of-plane reconfiguration problems. Equation (3) fixes the minimum number of maneuvers needed to meet a whatever set of end conditions for each subproblem. Concerning the out-of-plane reconfiguration, one has two equations in the two unknowns δv_n and u_M. Therefore, a total change of relative inclination vector of

$$
\Delta\delta\tilde{\boldsymbol{\alpha}}|_{\text{oop}} = a\delta\boldsymbol{i}_F - a\delta\boldsymbol{i}_0 = a\Delta\delta\boldsymbol{i} \tag{7}
$$

is produced by a maneuver placed at one mean argument of latitude u_j, which equals the phase angle of the total variation of the relative inclination vector [7,14,30]:

$$
u_j = \arctan\left(\frac{\Delta\delta i_y}{\Delta\delta i_x}\right) + k_j\pi, \qquad \delta v_N|_{\text{oop}} = v\|\Delta\delta\boldsymbol{i}\| \tag{8}
$$

In the in-plane reconfiguration problem, instead, one maneuver (the three unknowns δv_r, δv_t, and u_M) is not enough to satisfy all the four final aimed ROEs. In this case, a minimum of two maneuvers is required and a preference criterion can be introduced to rank all the feasible solutions. Because, generally, the minimization of the total delta-v expenditure is sought, in the following section, the assessment of the minimum possible cost of an in-plane reconfiguration is discussed.

III. Delta-v Lower Bound for In-Plane Reconfiguration Problem

The minimum possible delta-v cost for an in-plane reconfiguration derives straightaway from Eq. (3) and is independent from the number or type of the executed maneuvers. Specifically, it is given as the maximum among the following total variations of ROEs:

$$
\delta v|_{\text{ip}} \geq \max\left\{\frac{v}{2}\|\Delta\delta\boldsymbol{e}\|, \frac{v}{2}|\Delta\delta a^*|\right\} = V_{\text{LB}} \tag{9}
$$

where:

$$
|\Delta\delta a^*| = \max\{|\delta a_F - \delta a_0|, |\delta a^*_{\text{transf}} - \delta a_0|, |\delta a^*_{\text{transf}} - \delta a_F|\} \tag{10}
$$

and

$$
\delta a^*_{\text{transf}} = \frac{2}{3}|\Delta\delta\lambda|/\Delta u_{\max}
$$

is the minimum relative semimajor axis for accomplishing a given mean relative longitude transfer over the finite time to span $\Delta u_{\max}$. Equation (9) generalizes the expression addressed by [7,14,30],

because it includes the treatment of $\delta\lambda$. To the authors' knowledge, this case was only qualitatively mentioned in [32] when speaking about large longitude transfers. Equation (9) quantifies the qualitative distinction between reconfigurations that require a dominant change in the relative eccentricity vector from those that need a more relevant change in the generalized drift coefficient. In the first case, the relative motion changes mainly in the size of the relative orbit (i.e., $\|\Delta\delta\boldsymbol{e}\| > |\Delta\delta a^*|$). In the second case, it is more cost demanding either to correct the drift or to achieve the aimed mean longitude transfer.

The geometrical interpretation of the lower bound of the cost in terms of ROEs can be discussed with the aid of Fig. 1. Its left part depicts what happens in the relative eccentricity vector plane if a single tangential maneuver is performed to achieve an aimed variation $\Delta\delta\boldsymbol{e}$: the burn occurs at a mean argument of latitude equal to the phase angle of the total relative eccentricity vector variation. Similar to the $\delta\boldsymbol{i}$ case, the maneuver location is given by

$$u = \bar{u} + k\pi, \qquad \bar{u} = \arctan\left(\frac{\Delta\delta e_y}{\Delta\delta e_x}\right) \tag{11}$$

and the required delta-v is proportional to the length of $\Delta\delta\boldsymbol{e}$.

The right side of Fig. 1 depicts a reconfiguration in the $\delta\lambda/\delta a$ plane of the ROE space. Here the two points identify the initial and final conditions. The total variations to be achieved are $\Delta\delta\lambda$ and $\Delta\delta a$, respectively, along the axis x (i.e., local tangential direction) and y (i.e., local radial direction). According to the sketch, the initial configuration is characterized by $\delta a_0 < 0$, thus the deputy moves toward increasing $\delta\lambda$ (see straight line from zero, Fig. 1) as given by Eq. (2). To achieve $\delta\lambda_F$, a positive δa is needed to drift inward. The later the maneuver is performed, the greater the value of δa_{transf}, according to the gray-dotted line in the figure. Concerning the delta-v cost, both the contributions $\Delta\delta a$ and δa_{transf} are to be accounted for (i.e., bold-dashed arrow), in agreement with Eq. (10). Thin-solid lines represent movements performed for free due to the dynamics of the system. Nevertheless, it is here emphasized that a further expense is needed to fully satisfy the final conditions. After a Δu time interval, in fact, δa_F should be brought to its final value (i.e., zero in the figure). Therefore, in this case, the delta-v lower bound is minor compared with the achievable cost.

IV. In-Plane Reconfigurations with Two Maneuvers

This section analyses the solutions that can satisfy simultaneously an arbitrary set of final conditions through the minimum number of maneuvers. Previous works (i.e., SAFE [28], TAFF [29], ARGON [33]) exploited the analytical expression of a pair of tangential/radial maneuvers to accomplish the in-plane formation control. Despite their simplicity, these particular solutions can only establish three desired ROEs after the execution. As a consequence, multiple pairs of maneuvers and a dedicated guidance plan were necessary to complete the most general rendezvous.

Within our framework, the general expression of the in-plane reconfiguration in two maneuvers is

$$\mathbf{M}(u_F, u_1, \xi)\delta\mathbf{v} = n\Delta\delta\tilde{\boldsymbol{\alpha}} \tag{12}$$

where only the in-plane subparts of the matrices and vectors of Eq. (5) are considered. The final mean argument of latitude u_F is a parameter of the reconfiguration, u_1 is the mean argument of latitude of the first maneuver, and ξ represents the spacing between the two maneuvers according to $\xi = (u_2 - u_1) > 0$. Equation (12) is a system of four equations in six variables, namely two maneuver locations u_1, ξ and four delta-v magnitudes $\delta\mathbf{v}$. $\mathbf{M}$ is the following 2×2 matrix:

$$\mathbf{M} = \begin{pmatrix} 0 & 2 & 0 & 2 \\ -2 & -3(u_F - u_1) & -2 & -3(u_F - (u_1 + \xi)) \\ \sin u_1 & 2\cos u_1 & \sin(u_1 + \xi) & 2\cos(u_1 + \xi) \\ -\cos u_1 & 2\sin u_1 & -\cos(u_1 + \xi) & 2\sin(u_1 + \xi) \end{pmatrix} \tag{13}$$

which depends only on the angular variables and whose determinant depends only on ξ and is not null when $\xi \neq 0$. In the remainder of the paper, the following notations will be introduced:

$$n\Delta\delta\tilde{\boldsymbol{\alpha}}|_{\text{ip}} \overset{\text{def}}{=} n(\,\Delta\delta\tilde{a} \quad \Delta\delta\tilde{\lambda} \quad \Delta\delta\tilde{e}_x \quad \Delta\delta\tilde{e}_y)^T \overset{\text{not}}{=} (A \quad L \quad E \quad F)^T$$
$$\delta\mathbf{v} \overset{\text{def}}{=} (\,\delta v_{R1} \quad \delta v_{T1} \quad \delta v_{R2} \quad \delta v_{T2})^T \overset{\text{not}}{=} (x_1 \quad x_2 \quad x_3 \quad x_4)^T \tag{14}$$

If no delta-v minimization is sought, the analytical expression for the general two-impulse scheme via both tangential and radial burns as function of the maneuvers' locations (i.e., u_1 and ξ) and of the reconfiguration parameters (i.e., u_0 and u_F), for each given set of end conditions (i.e., $n\Delta\delta\tilde{\boldsymbol{\alpha}}$) is provided by

$$\delta\mathbf{v} = \frac{n}{|\mathbf{M}|}\tilde{\mathbf{M}}^T\Delta\delta\tilde{\boldsymbol{\alpha}} \tag{15}$$

where $|\mathbf{M}|$ and $\tilde{\mathbf{M}}$ are, respectively, the determinant and the adjugate matrix of $\mathbf{M}$. Because Eq. (15) takes into account the relationship between δa and $\delta\lambda$ [i.e., Eq. (2)], it generalizes the formulation in ([14] p. 44), at the cost of a less compact expression. Equation (15) is to be used every time that the constraints on the locations of the maneuvers are more significant than any delta-v minimization request.

From now on, though whenever possible, the delta-v minimization is taken into account for each feasible solution able to meet the complete set of ROEs at the final time. Such candidate solutions, together with their main characteristics, are summarized in Table 1, ranked via a reconfiguration identifier (i.e., last column). The "end conditions" column lists the eventual restrictions introduced on the aimed ROE set to obtain a solution of the problem within the related assumptions (i.e., "assumptions" columns).

As a first step, we consider an in-plane reconfiguration performed through a couple of pure tangential maneuvers (i.e., $x_1 = x_3 = 0$), in agreement with delta-v cost minimization treated in Sec. III. If the drift coefficient of the relative motion is not changed (i.e.,

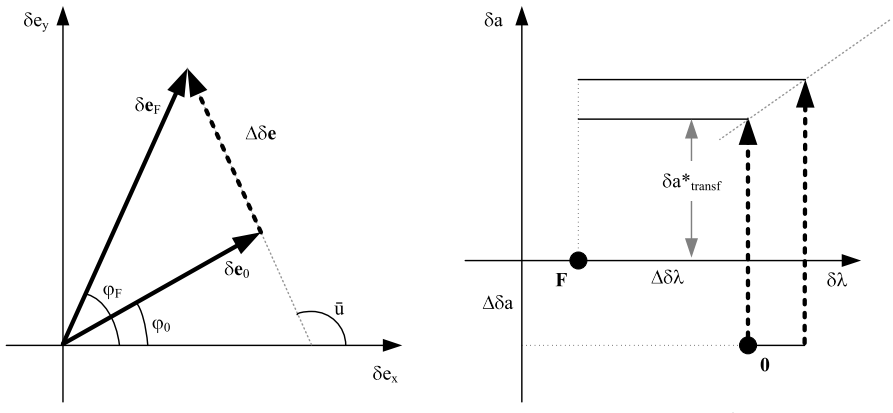

Fig. 1 In-plane reconfiguration in the relative eccentricity vector and $\delta\lambda/\delta a$ planes.

Table 1 Summary of existence and characteristics of double-impulse solutions for the in-plane reconfiguration

Assumptions					
Delta-v type	Locations	Degree of freedom	End conditions	Solution	Identifier ₦
T–T	u_1, ξ	4 eqt. 4 unk.	$\Delta\delta a = 0 \wedge \Delta\delta\lambda = 0$	$\nexists$	1
			$\Delta\delta a = 0 \wedge \Delta\delta\lambda \neq 0$	Numerical ξ^* $u_1^* = \bar{u} - \pi/2 - \xi^*/2$	2
			$\Delta\delta a \neq 0$	Numerical u_1^* and ξ^*	3
	$u_i = \bar{u} + k_i\pi$ $\{k_2 > k_1\} \in \mathbb{N}$	4 eqt. 4 unk.	$0 < \lvert\Delta\delta a^*\rvert < \lVert\Delta\delta\boldsymbol{e}\rVert$	Not acceptable $\{k_1 = k_2\} \notin \mathbb{N}$	4
	$u_1 = u_0$ $u_2 = u_F$	4 eqt. 2 unk.	$\lVert\Delta\delta\boldsymbol{e}\rVert \leq \lvert\Delta\delta a^*\rvert$	$\nexists$	5
R–R	u_1, ξ	3 eqt. 4 unk.	$\Delta\delta a = 0$	Analytical $\xi^* = \pi$ $u_1^* = \hat{u} + k\pi$	6
		4 eqt. 4 unk.	$\Delta\delta a \neq 0$	$\nexists$	7
RT–RT	u_1 $\xi = \pi$	4 eqt. 5 unk.	$\Delta\delta a = 0 \wedge \Delta\delta\lambda = 0$	Analytical u_1^* $u_1^* = \hat{u} + k\pi$	8
			$\Delta\delta a \neq 0$	Numerical u_1^*	9
	u_1, ξ	4 eqt. 6 unk.	$\Delta\delta a = 0 \wedge \Delta\delta\lambda = 0$	Numerical ξ^*	10
			$\Delta\delta a \neq 0 \vee \Delta\delta\lambda \neq 0$	Numerical u_1^* and ξ^*	11

Note: eqt. refers to equations, unk. refers to unknowns.

$\Delta\delta a = A = 0$), the magnitudes of the tangential maneuvers must be equal and opposite (i.e., $x_4 = -x_2$), and Eq. (12) becomes

$$\begin{cases} \xi x_4 = -L/3 \\ \tan\left(\frac{z}{2}\right) = -\frac{E}{F} \\ 2\,\sin\left(\frac{z}{2}\right)\sin\left(\frac{\xi}{2}\right)x_2 = E/2 \end{cases} \tag{16}$$

where $z = 2u_1 + \xi$. By recalling $\bar{u}$ from Eq. (11), $\arctan(-E/F) = \bar{u} - \pi/2$, thus the system is solved by

$$\sin\left(\frac{\xi}{2}\right)\left(\frac{4}{3}\frac{L}{E}\cos\,\bar{u}\right) = \xi \tag{17}$$

In the particular case where only the relative eccentricity vector of the initial configuration is changed (i.e., $\Delta\delta a = A = 0$, $\Delta\delta\lambda = L = 0$), Eq. (17) admits no solution with $\xi \neq 0$. This case is identified by ₦1 in Table 1. If $L \neq 0$, and if a numerical solution for ξ^* exists, then $u_1^* = \bar{u} - \pi/2 - \xi^*/2$ (see ₦2 in Table 1). Finally, ₦3 regards the general case in which a correction of the relative drift is required (i.e., $A \neq 0$). From Eq. (12), one can derive the delta-v magnitudes as a function of the locations of the maneuvers:

$$\begin{cases} x_2 = -\dfrac{3A(u_F - \xi^* - u_1^*) + 2L}{6\xi^*} \\ x_4 = \dfrac{3A(u_F - u_1^*) + 2L}{6\xi^*} \end{cases} \tag{18}$$

and the values u_1^* and ξ^* have to be computed numerically so that the final conditions on E and F are met. To solve the general double-tangential-impulse problem analytically, instead, one could try introducing some further assumptions on the specific locations of the maneuvers and computing the corresponding delta-v magnitudes from Eq. (18). Referring to Table 1, ₦4 and ₦5 impose constraints on the maneuvers' locations, motivated by the minimum delta-v principle, for the two possibilities of dominant change in relative eccentricity vector and in generalized drift. In the first case, the maneuvers are constrained to happen at $u_i = \bar{u} + k_i\pi$, as depicted Fig. 1; in the second one, the whole reconfiguration horizon is exploited. Nevertheless, both schemes do not lead to any solution, because they are not able to achieve the complete final ROE set.

As a second step, we consider an in-plane reconfiguration through a couple of pure radial maneuvers (i.e., $x_2 = x_4 = 0$). In the general case in which $\Delta\delta a \neq 0$, the reconfiguration admits no solution because the relative drift can be changed only by a tangential burn (see ₦7 in Table 1). If, instead, $\Delta\delta a = 0$, the number of effective equations reduces to three in the four unknowns: x_1, x_3, u_1, and ξ. Out of the infinite available solutions, the ones that minimize the delta-v cost, expressed as the magnitude of the delta-v vector, are characterized by $\xi^* = \pi$. The first maneuver is then located at

$$u_1^* = \hat{u} + k\pi, \qquad \hat{u} = \arctan\left(-\frac{\Delta\delta e_x}{\Delta\delta e_y}\right) = \bar{u} - \frac{\pi}{2} \tag{19}$$

with resultant minimum delta-v of magnitude:

$$|x_1| + |x_3| = v\left(\lVert\Delta\delta\boldsymbol{e}\rVert + \frac{\Delta\delta\lambda}{2}\right) \quad \text{if } \left(\lVert\Delta\delta\boldsymbol{e}\rVert - \frac{\Delta\delta\lambda}{2}\right) > 0 \tag{20}$$

This possible solution is identified by ₦6 in Table 1.

As a third and final step, no constraints on the typology of the two maneuvers are posed (see case RT–RT in Table 1). The particular case in which only the magnitude of the relative eccentricity vector is varied (i.e., $\Delta\delta a = 0 \wedge \Delta\delta\lambda = 0$) is treated in [26] where also the further condition of $\delta a_0 = 0$ is fixed. In that work, to follow an analytical approach, the constraint of $\xi = \xi^* = \pi$ is imposed, motivated by a numerical evidence accumulated over several simulations. According to our methodology, once fixed $\xi = \pi$, the same result can be easily obtained disregarding the value of δa_0, by observing that $x_4 = -x_2$ and $x_1 + x_3 = -(3/2)\pi x_2$. The magnitude of the delta-v vector is then minimized when $u_1^* = \hat{u} + k\pi$. According to Eq. (3), at these particular mean arguments of latitude, the tangential components of the delta-v are null. Thus, in this specific application (i.e., $\Delta\delta a = 0 \wedge \Delta\delta\lambda = 0$), where the maneuvers are imposed to be spaced by half-orbital period, the delta-v optimal double-impulse strategy is to perform a double radial burn and the correspondent cost is $v\lVert\Delta\delta\boldsymbol{e}\rVert$ m/s. This scenario is labeled as ₦8 in Table 1.

Our approach can be also used to treat a more general situation where any term between $\Delta\delta a$ or $\Delta\delta\lambda$ is not null. Nevertheless, because the cost functional is a transcendental function of u_1, its extrema have to be computed numerically (see ₦9, Table 1).

The last part of this third step deals with the case in which no constraints are posed on the angular variables u_1 and ξ. In this situation the delta-v minimum reconfiguration through two impulsive maneuvers has to be solved numerically disregarding the aimed end conditions. The solution that minimizes the functional cost $J = \delta\mathbf{v}^T\delta\mathbf{v}$ given Eq. (15), satisfies the following necessary conditions for optimality:

$$\frac{\partial J}{\partial u_1} = g_1(u_1, \xi) = 0 \quad \frac{\partial J}{\partial \xi} = g_2(u_1, \xi) = 0 \tag{21}$$

In analogy with the end conditions of ₦8 of Table 1 (i.e., $\Delta\delta a = 0 \wedge \Delta\delta\lambda = 0$), ₦10 represents the case in which only the relative eccentricity vector is changed. Thus, the functional cost becomes

$$J = M_1(\xi, E, F) + N_1(\xi, E, F)\,\sin\,u_1^2 + P_1(\xi, E, F)\,\sin\,2u_1 \tag{22}$$

where the expressions of M_1, N_1, and P_1 are given in the Appendix and the condition $g_1(u_1, \xi) = 0$ leads to $\tan\,2u_1 = -2P_1/N_1$. Such

expression is then substituted back in $g_2(\xi) = 0$, whose root ξ^* shall be found numerically.

In the most general case [i.e., $(A \neq 0 \vee L \neq 0) \wedge (E \neq 0 \vee F \neq 0)$], Eq. (21) constitutes a system of two nonlinear equations in the two unknowns u_1 and ξ (see №11 of Table 1). Among the possible available numerical methods, №11 can be solved through a multidimensional Newton–Raphson method with proper initial conditions.

According to Table 1, the feasible solutions of the bi-impulsive in-plane reconfiguration problem are marked with the identifiers 2, 3, and 6, and from 8 to 11. In this last part of the section, the delta-v costs achieved by these schemes are analyzed in the ROE space and compared with the in-plane lower bound cost [see Eq. (9)].

To this aim, the upper part of Fig. 2 depicts a sketch of the behavior of the №2 solution. For the sake of readability, the particular case in which $\delta a_0 = 0$ is shown. Because maneuvers are purely tangential, all the bold-dashed arrows have same lengths, proportional to $|x_2|$. Generally, the intermediate relative eccentricity vector achieved after the first maneuver constitutes the vertex of an isosceles triangle composed by the two arrows and the $\Delta\delta\boldsymbol{e}$ vector. This means that $u_1^* \neq \bar{u}$ and that the total delta-v cost is larger than $v\|\Delta\delta\boldsymbol{e}\|/2$. In the special conditions where the desired change of the mean relative longitude is

$$L = \pi \frac{3}{4} \frac{E}{\cos \bar{u}} \tag{23}$$

Eq. (17) gives $\xi^* = \pi$ and $u_1^* = \bar{u}$. Therefore, this reconfiguration provides the absolute minimum of the cost when $\|\Delta\delta\boldsymbol{e}\| > |\Delta\delta a^*|$. In all other cases, the lower bound is smaller than the achieved cost. It is emphasized that Eq. (23) expresses the obtainable $\delta\lambda_F$ if two tangential maneuvers are performed to satisfy three ROE end conditions sets of type $A = 0$ and arbitrary E and F (see SAFE [28] and TAFF [29]).

The bottom part of Fig. 2 shows №3. Since $\Delta\delta a \neq 0$, the two arrows have different lengths and $u_1^* \neq \bar{u}$. The condition $u_1^* = \bar{u}$, in fact, is identified by №4 in Table 1, which admits no solution.

Whenever the change in the generalized drift is the dominant factor (i.e., $\|\Delta\delta\boldsymbol{e}\| \leq |\Delta\delta a^*|$;), the cost achieved by №2 is always greater than or equal to the double of the lower bound, aiming to $\Delta\delta a = 0$ after having established a relative semimajor axis of minimum magnitude $\delta a^*_{\text{transf}}$. In the case of №3, instead, the minimum absolute delta-v might be reached if there exists a couple of impulses of same sign (i.e., $x_2 + x_4 = A/2$) so that $\delta a_0 < \delta a_{\text{tranf}} < \delta a_F$ and consistent with the aimed $\Delta\delta\boldsymbol{e}$.

№6 and №8 lead to exactly the same solution. The first was obtained by imposing a priori to burn only in the radial direction aiming at end conditions with $\Delta\delta a = 0$. The second does not introduce any assumption on the typology of the maneuver but constrains the impulses to be spaced by π and deals only with the specific end conditions of $\Delta\delta a = 0 \wedge \Delta\delta\lambda = 0$. Both gain a delta-$v$ cost of $v\|\Delta\delta\boldsymbol{e}\|$, which is exactly the double of the lower bound for the case $\|\Delta\delta\boldsymbol{e}\| > |\Delta\delta a^*|$. Indeed, they are both optimal solutions but, due to the constraints, the absolute minimum does not reside in the feasible space. №6 and №8 cannot be used when the generalized drift is the major change request by the reconfiguration, because this would not be compliant with the end conditions (№8), nor with the existence conditions of Eq. (20) (№6).

№10 and №11 represent the generalization of the cases №8 and №9, having removed the assumption of $\xi = \pi$, and the following qualitative considerations can be stated. When $\|\Delta\delta\boldsymbol{e}\| > |\Delta\delta a^*|$, the cost achieved for both these schemes is larger than the lower bound as the radial components of the maneuvers are not null. Otherwise, №10 would correspond to №1, which admits no solution, and №11 would correspond to №3, which always spends more than the lower bound. If $\|\Delta\delta\boldsymbol{e}\| \leq |\Delta\delta a^*|$, instead, only №11 is applicable and its cost is greater than the lower bound whenever the radial components are not completely null.

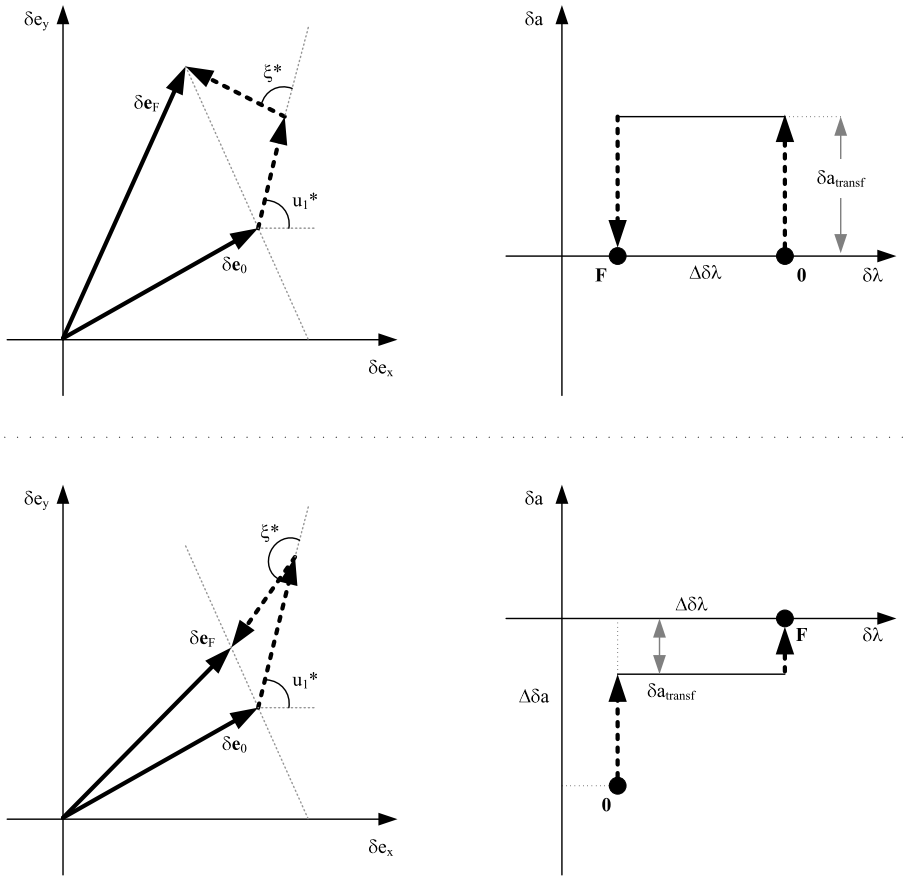

Fig. 2 Sketch on the ROE space views of №2 (top) and №3 (bottom).

V. In-Plane Reconfigurations with Three Maneuvers

This section addresses the characteristics of the solutions of the in-plane reconfiguration problem when three impulsive maneuvers are executed. According to our framework, the general reconfiguration is written as

$$\mathbf{M}(u_F, u_1, u_2, u_3)\delta\mathbf{v} = n\Delta\delta\tilde{\boldsymbol{\alpha}} \tag{24}$$

where now $\delta\mathbf{v} = (x_1, x_2, x_3, x_4, x_5, x_6)^T$. Thus, nine unknowns can be exploited to meet the four equations expressing the end conditions at the final time. To find delta-v minimum solutions, we can reduce the search space by imposing to use tangential burns only (i.e., $x_1 = x_3 = x_5 = 0$), as suggested in Sec. III. At this stage, however, the whole congruence of the problem, which was not taken into account at that time, has to be verified.

When no radial components are used, the number of unknowns is reduced to six and the feasible solution schemes are summarized in Table 2. ₦14 represents the general case in which the three locations of the maneuvers are free to assume whatever value in their domain. Thus, the delta-v magnitudes that guarantee the satisfaction of three of the end conditions can be derived from Eq. (24) as $x_i = f(u_1, \xi_1, \xi_2)$, where $\xi_1 = u_2 - u_1$, $\xi_2 = u_3 - u_1$ and $\xi_2 > \xi_1$. Then, the solution that minimizes the magnitude of the delta-v vector has to satisfy also the remaining end conditions expressed by

$$\tan u_1 = \frac{F\hat{a} - E\hat{b}}{E\hat{a} + F\hat{b}} \quad \text{where} \quad \begin{matrix} \hat{a} = x_2 + \cos\xi_1 x_4 + \cos\xi_2 x_6 \\ \hat{b} = \sin\xi_1 x_4 + \sin\xi_2 x_6 \end{matrix} \tag{25}$$

which is a transcendental function in u_1 and requires a numerical solution.

As performed for the double-impulses case, some further assumptions on the locations of the maneuvers can be introduced to simplify the search of a possible analytical solution. ₦12 in Table 2 reports the case in which the spacing between the maneuvers is constrained. Accordingly, the maneuvers must occur at multiples of half the orbital period $k_i\pi$ of a variable argument of latitude $\tilde{u}$ and the multiplication coefficients are chosen so that $k_1 < k_2 < k_3$ and $k_i \in \mathbb{N}$. Given these assumptions, the imposition of three end conditions determines that the angle $\tilde{u}$ is exactly the phase of the total variation of the relative eccentricity vector $\Delta\delta\boldsymbol{e}$, so far referred to as $\bar{u}$ [see Eq. (11)], disregarding the values assumed by k_i. Therefore, maneuvers are located at arguments of latitude $\bar{u} + k_i\pi$, as suggested by the results presented in [7,30,32], where these locations were chosen as necessary conditions of the delta-v minimization problem when the change in the shape of the relative orbit was the dominant correction to be applied by the reconfiguration.

Once computed $\bar{u}$, the values of the delta-v magnitudes can be analytically derived through three of Eq. (24), obtaining $x_i = f(k_1, k_2, k_3)$ for whatever required change of ROEs. In particular, being k_i natural numbers and being the transfer over a limited time, there exists a finite set of admissible combinations of k_i, though characterized by different delta-v costs. The finite set of feasible analytical solutions can be systematically computed using the formulations grouped in Tables 3 and 4, where

$$q = u_F - \bar{u} - k_1\pi, \qquad p = u_F - \bar{u} - k_2\pi, \qquad l = u_F - \bar{u} - k_3\pi \tag{26}$$

₦13 in Table 2, instead, applies some constraints directly on the values of some of the locations of the maneuvers u_i. Such a strong assumption is motivated by the fact that, in some reconfigurations, it is convenient to perform the first and the last maneuvers, respectively, as soon and as late as possible (i.e., $u_1 = u_0$ and $u_3 = u_F$) to exploit at maximum the transfer time. In this situation, Eq. (24) reduces to a system of four equations in four unknowns, and the location of the intermediate maneuver is determined by the satisfaction of the end conditions

$$u_2 = \tilde{K}(u_0, u_F, A, L, E, F)\cos u_2 + \tilde{P}(u_0, u_F, A, L, E, F)\sin u_2 + \tilde{Q}(u_0, u_F, A, L, E, F) \tag{27}$$

where the expressions of $\tilde{K}$, $\tilde{P}$, and $\tilde{Q}$ are given in the Appendix. Equation (27) admits several solutions, whenever $|\tilde{Q}|$ is smaller than the amplitude of the periodical part in u_2. These solutions can be numerically found in a few iterations of a Newton method by assuming initial conditions in proximity of the extrema of the second

Table 2 Summary of the characteristics of triple-tangential-impulse solutions for the in-plane reconfiguration

Assumptions				
Delta-v type	Locations	Degree of freedom	Solution	Identifier ₦
T–T–T	$u_i = \tilde{u} + k_i\pi$	4 eqt. 7 unk.	Analytical	12
	$\{k_1 < k_2 < k_3\} \in \mathbb{N}$		$\tilde{u}^* = \bar{u}$, $k_i \in \mathbb{N}$	
	$u_1 = u_0$	4 eqt. 4 unk.	Numerical u_2^*	13
	$u_3 = u_F$			
	u_1, u_2, u_3	4 eqt. 6 unk.	Numerical u_i^*	14

Note: eqt. refers to equations, unk. refers to unknowns.

Table 3 Structure of solution scheme ₦12

Aimed end conditions			Signs of $\cos u_i$ and $\sin u_i$ from Eq. (24)	
	B	b	$+--/---+/--+-$	$+-+/++-/-++$
$\bar{u} \in [0, \pi/2)$	E	$\cos\bar{u}$	$\tilde{x} = \frac{bA+B}{4b}$	$\tilde{x} = \frac{bA-B}{4b}$
$\bar{u} = \pi/2$	F	$\sin\bar{u}$		
$^*\bar{u} \in (\pi/2, \pi)$	E	$\lvert\cos\bar{u}\rvert$	$\tilde{x} = \frac{bA-B}{4b}$	$\tilde{x} = \frac{bA+B}{4b}$

Table 4 All possible delta-v expressions for solution scheme ₦12

Signs	$\tilde{x} = \frac{bA \pm B}{4b}$	D	Remaining delta-v expressions
$+--$	$x_2 = \tilde{x}$	$12b(p-l)$	$x_4 = -(4bL \pm 3(q-l)B + 3b(q+l)A)/D$
$-++$			$x_6 = +(4bL \pm 3(q-p)B + 3b(q+p)A)/D$
$--+$	$x_6 = \tilde{x}$	$12b(q-p)$	$x_2 = -(4bL \mp 3(p-l)B + 3b(p+l)A)/D$
$++-$			$x_4 = +(4bL \mp 3(q-l)B + 3b(q+l)A)/D$
$-+-$	$x_4 = \tilde{x}$	$12b(q-l)$	$x_2 = -(4bL \pm 3(p-l)B + 3b(p+l)A)/D$
$+-+$			$x_6 = +(4bL \mp 3(q-p)B + 3b(q+p)A)/D$

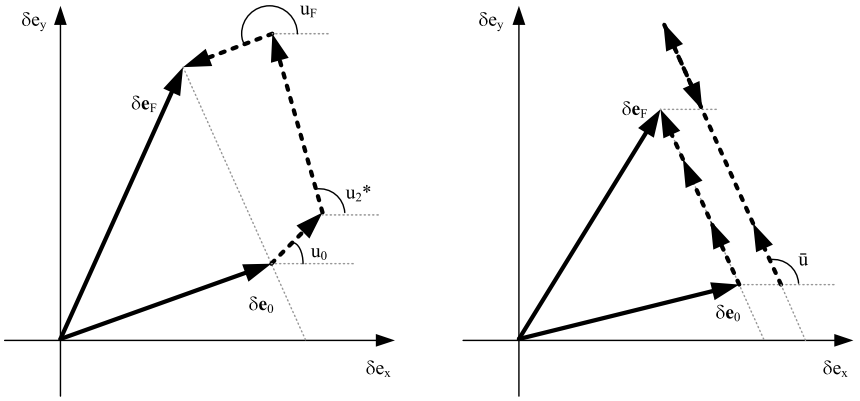

Fig. 3 Sketches in the δe plane for the three tangential maneuvers reconfiguration.

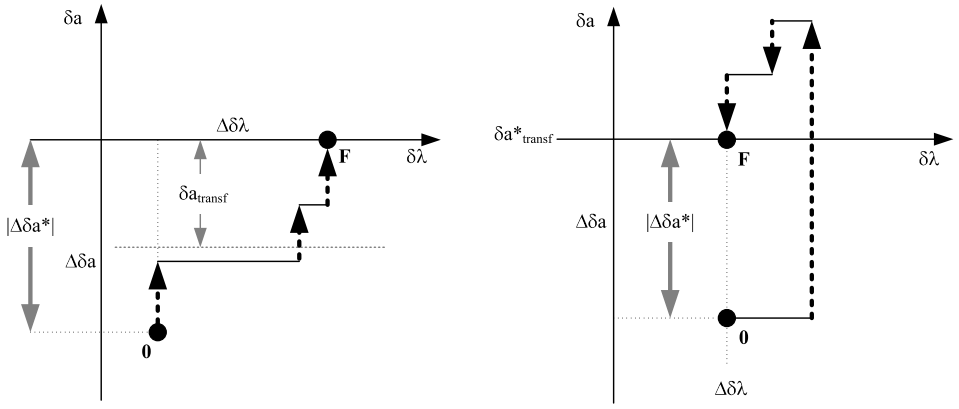

Fig. 4 Sketches in the $\delta\lambda/\delta a$ plane for the three tangential maneuvers reconfiguration.

member of Eq. (27). Once known u_2^*, the delta-v magnitudes are again computed in closed form, since $x_i = f(u_2^*, u_0, u_F, A, L, E, F)$. The finite set of possible solutions of Eq. (27) with $u_0 < u_2^* < u_F$ is characterized by different delta-v costs.

This last part of the section addresses how the feasible solutions of the in-plane reconfiguration problem through three tangential burns behave in terms of the achieved delta-v cost. Because these schemes exploit only tangential maneuvers, they are all candidates to achieve the lower bound cost. Differences rely on how the locations of the maneuvers are computed and how the subsequent delta-v magnitudes are derived to meet the end conditions. Here, a qualitative analysis is performed based on the geometrical meaning of the ROEs in their space, to assess the implications of the problem's consistency. In agreement with the previous discussion, the two cases of dominant change in the magnitude of the relative eccentricity vector and in the magnitude of the generalized drift are discussed.

Let us consider the case in which the reconfiguration asks for $\|\Delta\delta\boldsymbol{e}\| > |\Delta\delta a^*|$. Then the cost driver is the behavior in the relative eccentricity vector plane and Fig. 3 illustrates possible situations that might occur. The behavior of ₦13 and ₦14 is depicted in the left view. In the first case, this happens whenever the provided u_0 and u_F have not same modulus-π of $\bar{u}$. Concerning ₦14, this occurs whenever the solution found is a local minimum with $u_i(\mathrm{mod}\ \pi) \neq \bar{u}(\mathrm{mod}\ \pi)$. In both situations, the delta-v achieved is greater than the lower bound, because the sum of the length of the bold-dashed arrows is greater than $\|\Delta\delta\boldsymbol{e}\|$. The right part of Fig. 3 deals with the options in which all maneuvers occur at some arguments of latitude whose modulus-π equals the one of $\bar{u}$ (i.e., ₦12). Here, the changes in the relative eccentricity vector always lay parallel to the vector $\delta\boldsymbol{e}_F - \delta\boldsymbol{e}_0$. The absolute minimum is achieved whenever the covered total length is equal to $\|\Delta\delta\boldsymbol{e}\|$. This happens if all the intermediate relative eccentricity vector corrections are directed as the total aimed $\Delta\delta\boldsymbol{e}$ variation, leading to the following delta-v minimum criterion for the ₦12 solution scheme:

$$(\Delta\delta\hat{\boldsymbol{e}}|_{\tilde{x}}^T \Delta\delta\hat{\boldsymbol{e}}|_{\mathrm{tot}} > 0) \wedge (\Delta\delta\hat{\boldsymbol{e}}|_{j1}^T \Delta\delta\hat{\boldsymbol{e}}|_{j2} > 0) \wedge (\Delta\delta\hat{\boldsymbol{e}}|_{j1}^T \Delta\delta\hat{\boldsymbol{e}}|_{\mathrm{tot}} > 0) \tag{28}$$

where $\hat{\bullet}$ indicates unit vectors, $\tilde{x}$ is defined in Table 3, and $j1$ and $j2$ represent the first and second remaining tangential burns.

Finally, let us consider the remaining case in which the reconfiguration asks for $\|\Delta\delta\boldsymbol{e}\| \leq |\Delta\delta a^*|$. Here, the behavior in the $\delta\lambda/\delta a$ plane drives the cost, and, being all the maneuvers purely tangential, the delta-v cost is given by the sum of all the vertical movements that take place. Geometrically, the lower bound corresponds to the length of $|\Delta\delta a^*|$.

To understand the structure of the feasible solutions, one should consider the satisfaction of the end conditions in δa and $\delta\lambda$. Whenever $A > 0 \wedge L < 0$ or $A < 0 \wedge L > 0$, the end conditions might be satisfied by three $\Delta\delta a$ corrections in the same direction. An example of this situation is depicted in the left view of Fig. 4. There $\delta a_0 \leq \delta a^*_{\mathrm{transf}} < \delta a_F$ and maneuvers are distributed so that a drift is first established and then stepwise reduced until $\delta\lambda_F$ is achieved. If such a

Table 5 List of numerical examples of in-plane reconfigurations

	Relative orbits description									
Example	$\delta\boldsymbol{\alpha}_0$, m				$\delta\boldsymbol{\alpha}_F$, m				Solution scheme	Case
$E1$	0	−10,000	200	−10	0	−10,000	230	50	8/10/12/13/14	only $\|\Delta\delta\boldsymbol{e}\| \neq 0$
$E2$	50	−10,000	230	−50	0	−9,800	150	0	3/9/11/12/13/14	$\|\Delta\delta\boldsymbol{e}\| > \|\Delta\delta a^*\|$

Table 6 Comparison of the results of the reconfiguration $E1$ of Table 5

Solution №	u_1, rad	u_2, rad	u_3, rad	δv_{R1}, m/s	δv_{T1}, m/s	δv_{R2}, m/s	δv_{T2}, m/s	δv_{T3}, m/s	δv, m/s
8	5.8195	8.9611	—	−0.0352	0.0000	0.0352	0.0000	—	0.0704
10	0.0766	5.2793	—	−0.0314	0.0080	−0.0314	−0.0080	—	0.0649
12	4.2487	7.3903	10.5319	—	−0.0088	—	0.0176	−0.0088	0.0352
13	0.0000	4.6253	15.7080	—	0.0223	—	−0.0316	0.0093	0.0632

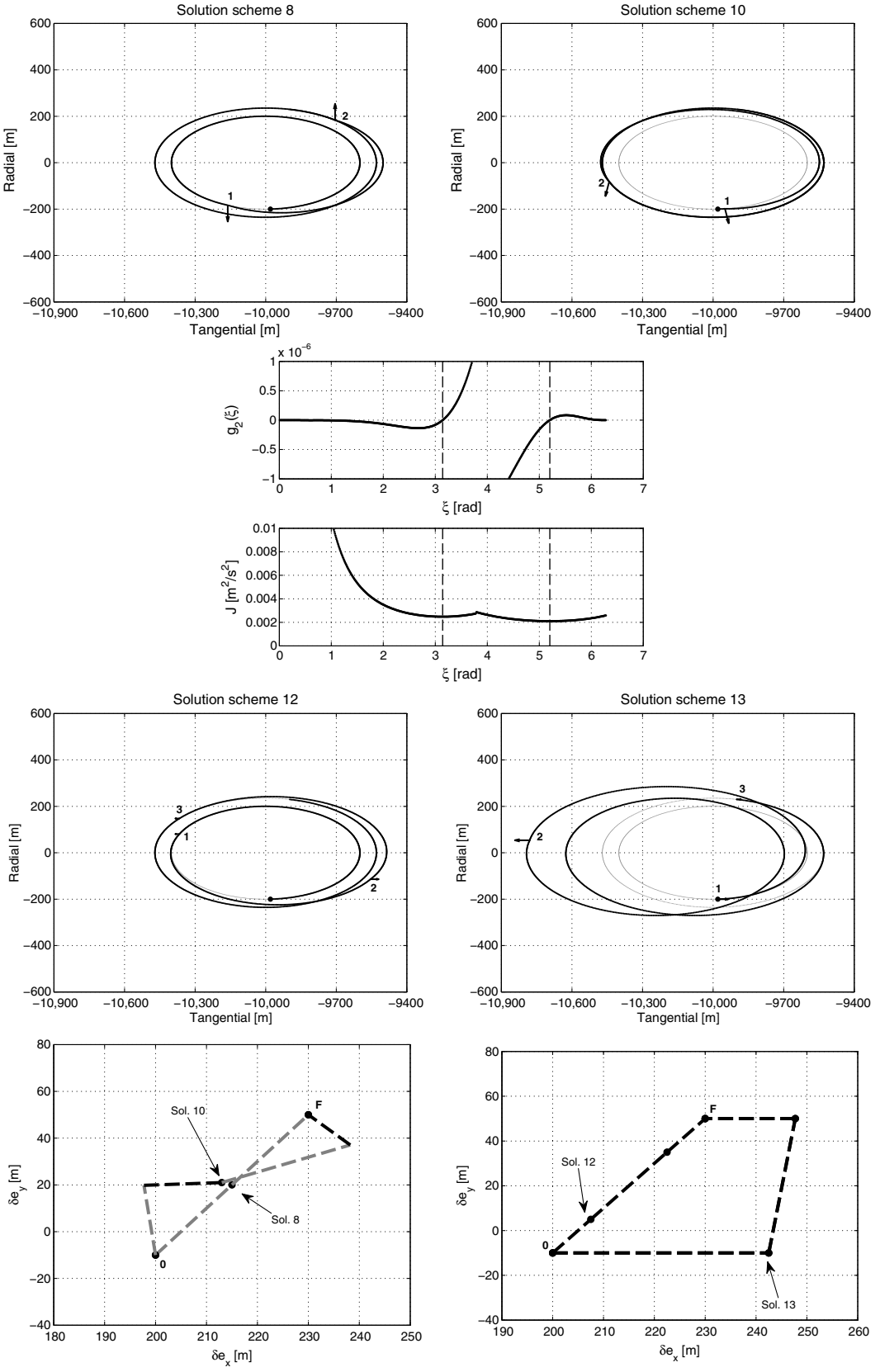

Fig. 5 Possible reconfiguration solutions for $E1$.

solution exists, then its minimum cost would be equal to the lower bound. Regarding all other possible combinations of aimed A and L corrections, the congruence requires at least a delta-v of different sign. In these cases, the minimum achievable delta-v cost is greater than the lower bound because the displacement $|\Delta\delta a^*|$ is covered by arrows of both directions. An example of this situation is depicted in the right view of Fig. 4, where the reconfiguration aims at $\Delta\delta\lambda = 0$ (i.e., $\delta a^*_{\text{transf}} = 0$) and no drift.

VI. Examples of In-Plane Reconfigurations

In this section, some numerical examples of the aforementioned solutions are produced. In particular, two scenarios have been chosen to represent a transfer between two bounded orbits (i.e., $E1$) and a reconfiguration where all the in-plane ROEs change, with dominant correction in the relative eccentricity vector (i.e., $E2$). Table 5 lists both considered examples, where each reconfiguration is described in terms of initial and final relative orbits. The "case" column highlights the category's affiliation. The applicable solution schemes, instead, are recalled through the identifier of Tables 1 and 2 in the "solution scheme" column.

In agreement with the characteristics of the employed model of relative dynamics (see Sec. II), some assumptions on the chief absolute orbit need to be fixed, without affecting the generality of the presented results. In particular, the chief spacecraft orbit is assumed to be circular at 750 km altitude and the reconfigurations have to occur in 2.5 orbital periods, starting with the deputy satellite at the ascending node (i.e., $u_0 = 0$ and $u_F = 5\pi$).

The first example (i.e., $E1$) deals with the case when a transfer between two bounded relative orbits is performed, and only the relative eccentricity vector of the formation is changed. Results in terms of maneuvers' locations and magnitudes are summarized in Table 6. According to Table 1, only the approaches ₦6, ₦8, and ₦10 are available. Since $A = 0 \wedge L = 0$, ₦6 and ₦8 achieve the same solution characterized by two analytically computed radial burns. ₦10 numerically computes the maneuver spacing ξ that minimizes the cost function of Eq. (22) by finding the roots of g_2 [see Eq. (21)] through a Newton method and uses such value to determine u_1. From Table 2, the schemes ₦12 and ₦13 are considered. The optimal locations computed by ₦12 coincide with the ones identified in [7,30], because $E1$ involves $\Delta\delta a = \Delta\delta\lambda = 0$. As expected due to its construction, the first and last maneuvers of ₦13 occur at the start and end of the maneuvering horizon.

Figure 5 collects some visualizations related to $E1$. The views in the radial–tangential frame show the in-plane trajectories performed during the reconfiguration. The initial and final aimed relative orbits are plotted in light gray. The transfer is marked in black, starting from a dot representing the relative position at u_0. The instantaneous delta-v are depicted on the trajectory at their correspondent maneuvers' locations. Direction and sizes are compliant with their current values, though scaled by a factor of 2000 to make them visible in all the plots presented across the paper. To ease the comprehension of the results, the delta-v vectors are labeled with the indices that appear in the results tables related to each example treated. The second-central view of Fig. 5 depicts the behavior of J as function of the spacing between the maneuvers ξ. It can be noted that the value $\xi = \pi$ (exploited in [26] and assumed in ₦8 as a hypothesis) constitutes a local minimum of the function. In this case, having relaxed the constraint over ξ allows finding the solution $\xi = 5.2027$ rad that corresponds to the absolute minimum of the cost function. Thus, the solution scheme ₦10 generalizes ₦8. The results in terms of delta-v cost can be geometrically visualized in the relative eccentricity plane (i.e., bottom views of Fig. 5). Initial and final relative eccentricity vectors are labeled with zero and F. The ROE variations are bold-dashed segments in gray or in black if due to radial or tangential components respectively. The solution scheme ₦8 brings $\delta\boldsymbol{e}$ to its final value along the direction of the total aimed variation $\Delta\delta\boldsymbol{e}$, in accordance with Eq. (19). Being $\hat{u} = \bar{u} - \pi/2$, the tangential components are null (i.e., the segments are both gray) and the cost achieved is the double of the lower bound that amounts to 0.0352 m/s. Solution ₦10 is cheaper, thanks to the fact that also exploits some tangential burns to accomplish the reconfiguration. ₦12 moves the relative eccentricity vector from zero to F in two steps along the $\Delta\delta\boldsymbol{e}$ direction. The obtained delta-v cost coincides with the value of the lower bound. Within the transfer time of $E1$, it was possible to identify only one optimal solution, which satisfies Eq. (28). The cost of ₦13 is clearly greater than the lower bound because the modulus-π values of u_0 and u_F are zero. This is shown graphically in the relative eccentricity vector plane, where the changes caused by the first and last maneuvers are depicted via horizontal dashed-bold segments. The remaining middle maneuver is selected as the option among the feasible ones that realizes the minimum path toward F.

The results obtained for the example $E2$ are summarized in Table 7; corresponding trajectories and ROE views are depicted in Figs. 6 and 7. The schemes ₦12 and ₦13 have been used over two different transfer times: the fastest option lasts again 2.5 orbital periods, whereas the other one involves 7.5 chief's revolutions to achieve the final aimed condition. The applicable two-maneuver solution schemes to perform the $E2$ reconfiguration are ₦3, ₦9, and ₦11. ₦3 numerically computes the unique solution achievable through two tangential burns. Scheme ₦9 searches for the value of u_1 correspondent to the minimum of the magnitude of the delta-v vector, being ξ fixed by construction. Method ₦11 instead needs to solve a nonlinear system in the two unknowns u_1 and ξ, with proper initial conditions here detected thorough an extensive search process. The best obtained solution corresponds to the values reported in Table 7 and achieved the best performance among the double-impulse solution schemes. Nevertheless, for $E2$, the value of the in-plane delta-v lower bound amounts to 0.0495 m/s and it is achieved only by ₦12 during the longest transfer time.

The motivation of the difference in cost between the various solutions can be visualized in the relative eccentricity vector plane views, where the total length of the dashed segments is proportional to the delta-v value. The cost obtained by ₦9 is remarkably greater than the others, because mainly radial maneuvers are used to accomplish the ROE corrections, due to the imposition of a fixed value of ξ. This resembles the behavior of ₦8 for the case when $\Delta\delta a$ and $\Delta\delta\lambda$ were zero. Despite the double cost of gray segments as compared with black ones of same length, the exploitation of two small radial components allows ₦11 to achieve an overall shorter length with respect to the path drawn by ₦3. Regarding the triple-impulse schemes, when only 2.5 orbits are used to perform the reconfiguration, the best option offered by ₦12 is suboptimal because its correction exceeds the $\Delta\delta\boldsymbol{e}$ segment. In this situation, scheme ₦13 scores a better result. By allowing more transfer time, instead, ₦12 identifies multiple feasible optimal solutions (i.e., 23 options), among which is the one of Fig. 7.

Table 7 Comparison of the results of the reconfiguration $E2$ of Table 5

Duration, orbits	Solution	u_1, rad	u_2, rad	u_3, rad	δv_{R1}, m/s	δv_{T1}, m/s	δv_{R2}, m/s	δv_{T2}, m/s	δv_{T3}, m/s	δv, m/s
2.5	3	5.0951	10.4950	—	0.0000	−0.0640	0.0000	0.0377	—	0.1017
	9	5.1246	8.2662	—	−0.1082	−0.0336	−0.1641	0.0073	—	0.2776
	11	0.3560	13.2947	—	−0.0574	−0.0283	−0.0210	0.0021	—	0.0851
	12	2.5830	5.7246	15.1494	—	−0.0088	—	−0.0379	0.0204	0.0671
	13	0.0000	5.2888	15.7080	—	−0.0099	—	−0.0313	0.0150	0.0562
7.5	12	2.5830	5.7246	46.5653	—	0.0058	—	−0.0379	0.0058	0.0495
	13	0.0000	23.9983	47.1239	—	−0.0135	—	−0.0290	0.0162	0.0587

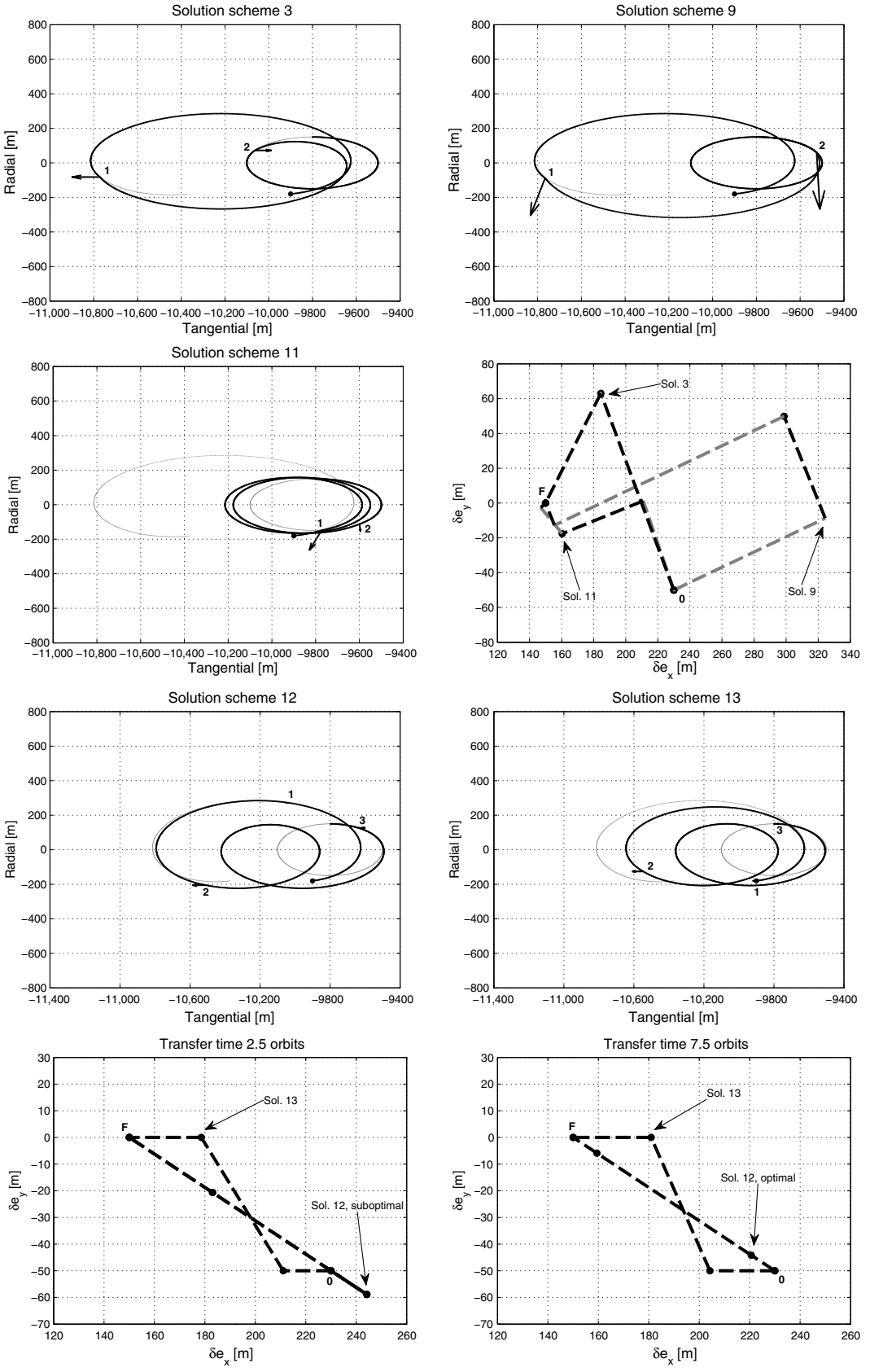

Fig. 6 Possible reconfiguration solutions for $E2$.

VII. Final Guidelines for a Maneuver Planner

This section is meant to provide an operational summary of the results presented across this paper. According to our framework, a formation reconfiguration consists in achieving a user-defined complete set of ROEs in a defined finite time interval. It is emphasized that this simple approach can also be exploited in realistic operational scenarios, where large reconfigurations have to be accomplished over wide time horizons and where time constraints limit when to schedule the maneuvers. The overall reconfiguration, in fact, can be expressed as a sequence of intermediate ROE sets to be

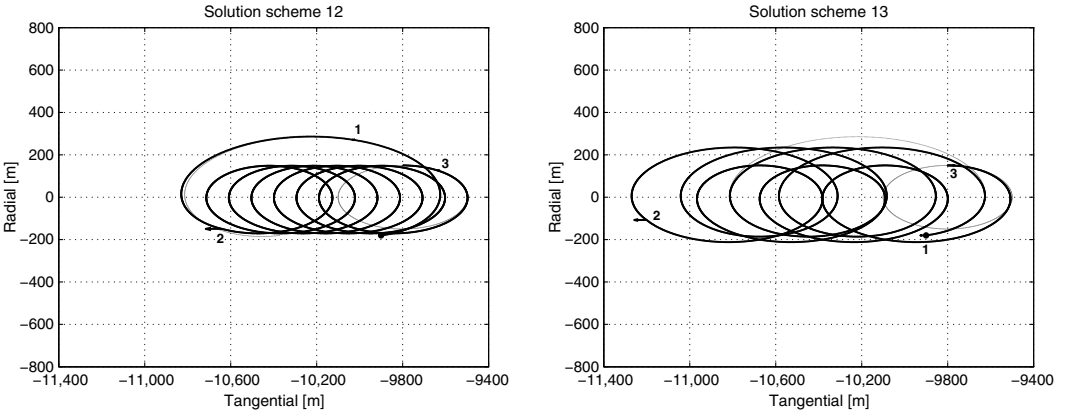

Fig. 7 Reconfiguration trajectories for $E2$ via ₦12 and ₦13 over 7.5 chief's orbits.

achieved at certain times to fulfill any high-level strategy that accounts for the proper exploitation of the timeline [31].

The decision process to select a reconfiguration strategy, given a certain application scenario, is depicted in Fig. 8. Out-of-plane and in-plane corrections are decoupled and the latter problem can be solved in multiple ways. This study focused exclusively on solution schemes able to satisfy the complete set of in-plane end conditions at the final time. Consequently, Fig. 8 lists all the suitable solution methods depending on the end conditions' formulation of each application scenario. Graphically, they are reported in order of decreasing level of generality.

The further step of the selection process has to be accomplished taking into account case-specific design drivers. Operational relevant features are listed in the dashed box of Fig. 8. They concern thrusters' duty cycle, for activities that involve several reconfigurations over long time periods. Attitude constraints might prevent performing maneuvers due to instrument and communication pointing requirements. Passive safety is a major requirement during proximity and final rendezvous phases. In case of employment of visual-based relative navigation techniques, visibility constraints might also become relevant, to avoid the target exiting the instrument's field of view. Generally, determinism and predictability are important features for accomplishing the maneuver planning onboard. These regard the easiness to compute the required maneuvers and the assessment of the ROE configurations and maneuvers' locations after each intermediate phase of the reconfiguration. Finally, the minimization of the delta-v expenditure can also constitute a driver.

Table 8 summarizes all the meaningful characteristics, according to the design drivers mentioned in Fig. 8, for each available solution method. The two-maneuver option generally requires to be solved through a numerical method with proper initial conditions. Despite this computational effort, the double-tangential option cannot achieve the absolute minimum of the delta-v cost when the change in the size of the formation is the dominant cost factor, except in the special case of ₦2 and L given by Eq. (23). Moreover, the location of the intermediate $\delta\boldsymbol{e}$ is difficult to be predicted. On the other hand, the numerical solutions of types ₦9–₦11 involve the use of maneuvers with no null radial components, and hence are always more expensive than the lower bound cost. The available two-maneuver delta-v minimum purely analytical schemes apply only to specific scenarios and achieve a suboptimal cost, because they employ couples of radial burns due to the maneuvers' spacing constraint (i.e., ₦6/8 in Table 8).

The triple-tangential maneuvers' scheme allows finding multiple analytical (i.e., ₦12) or semi-analytical solutions (i.e., ₦13) for whatever aimed final ROE set. When the variation of $\Delta\delta\boldsymbol{e}$ is the dominant cost factor and the reconfiguration time is enough, this scheme can fulfill the absolute minimum possible delta-v cost. On the other hand, when the available time is limited (i.e., $E2$ on the short transfer horizon) or when a reconfiguration asks for a prevalent variation in the generalized drift $\Delta\delta a^*$, it can be more cost convenient to exploit ₦13, hence starting and stopping the drift, respectively, as first and last as possible action. Both these methodologies offer multiple solutions over a reconfiguration window, and ₦12 can provide multiple delta-v equivalent options. This aspect is fruitful for the management of time constraints to improve the approach suggested in [32]. Instead of moving the optimal mean argument of latitude of a maneuver outside a forbidden zone, other available cost-equivalent solutions can be selected, without accounting for an increment of the delta-v expenditure.

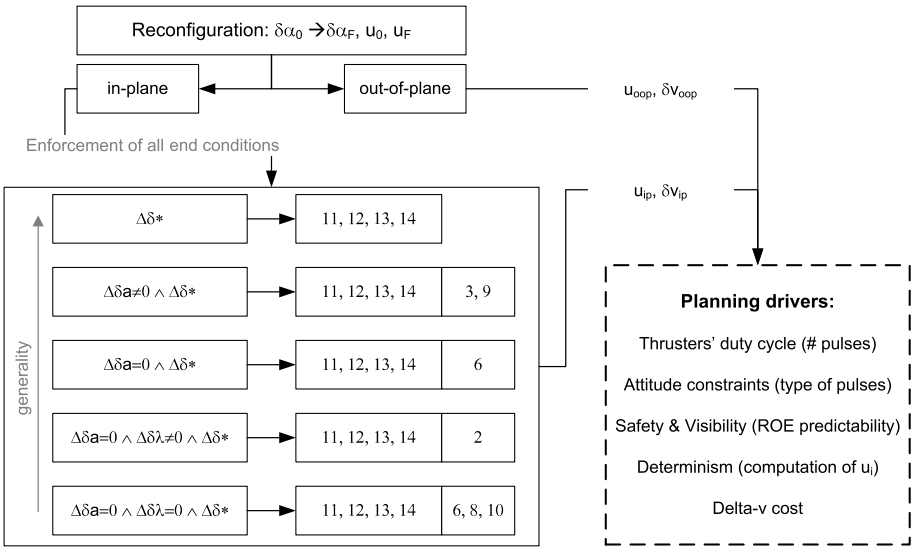

Fig. 8 Decision process's chart to select a proper solution scheme.

Table 8 Main characteristics of the feasible in-plane maneuvering schemes presented so far

	Determinism		Maneuvers			Delta-v cost	
Identifier ₦	(Semi) analytical	Numerical	No.	Type	ROE predictability	$\|\Delta\delta\boldsymbol{e}\| > \|\Delta\delta a^*\|$	$\|\Delta\delta\boldsymbol{e}\| \leq \|\Delta\delta a^*\|$
2		x	2	T	No	$\geq V_{\mathrm{LB}}$	$\geq 2V_{\mathrm{LB}}$
3		x	2	T	No	$> V_{\mathrm{LB}}$	$\geq V_{\mathrm{LB}}$
6	x		2	R	Yes	$2V_{\mathrm{LB}}$	N.A.
8	x		2	RT	Yes	$2V_{\mathrm{LB}}$	N.A.
9		x	2	RT	No	$> V_{\mathrm{LB}}$	$> V_{\mathrm{LB}}$
10		x	2	RT	No	$> V_{\mathrm{LB}}$	N.A.
11		x	2	RT	No	$> V_{\mathrm{LB}}$	$\geq V_{\mathrm{LB}}$
12	x		3	T	Yes	$\geq V_{\mathrm{LB}}$	$\geq V_{\mathrm{LB}}$
13	x		3	T	Partial	$\geq V_{\mathrm{LB}}$	$\geq V_{\mathrm{LB}}$
14		x	3	T	No	$\geq V_{\mathrm{LB}}$	$\geq V_{\mathrm{LB}}$

An example of application of the guidelines here discussed is provided by [31], where the design of the maneuver planner for the Autonomous Vision Approach Navigation and Target Identification Experiment, to be conducted in the frame of the DLR FireBird mission, is addressed. There, the intermediate reconfigurations prescribed by the high-level guidance are performed via the ₦12 solution scheme. In this case, in fact, the onboard autonomy required the maximum available level of determinism and predictability. Moreover, ₦12 is compatible with the maneuvers' spacing constraint, imposed to slew the one-direction thrusters' system in any appropriate direction. Finally, ₦12 together with out-of-plane corrections also satisfy the communication attitude constraints that require the satellite to keep two axes in the T–N plane during ground contacts.

VIII. Conclusions

This work addressed the strategy to perform a formation reconfiguration, with respect to a chief satellite on an almost circular orbit, through a limited number of impulsive maneuvers. Without loss of generality, the reconfiguration is accomplished on a finite time interval. Whereas the approach of involving a limited number of maneuvers is motivated on the one hand by the preference to exploit analytical or semi-analytical solution methods, on the other hand, it is motivated by the attempt to spend the minimum possible delta-v.

The relative dynamics is parameterized through relative orbital elements. This choice is driven by the straight meaning that these parameters possess in describing the characteristics of the relative orbit. Moreover, this allowed setting up a general framework in which several reconfiguration strategies have been systematically searched and discussed. As a result, all the maneuvering schemes able to satisfy at the final time the complete set of end conditions through two and three burns have been categorized. Feasible strategies have been ordered according to the application scenarios (i.e., specific end conditions) they can deal with. This allowed recognizing and comparing case-specific methodologies previously published in the literature. Their range of applicability has been discussed and, in some cases, strategies able to generalize their solutions have been proposed.

Besides the application scenarios, other significant characteristics of the reconfiguration strategies have been taken into account. Special focus, in fact, has been given to the determinism of a maneuvering scheme. This concerns the easiness of computing magnitudes and locations of the required maneuvers. Among the available possibilities, simple and practical solution schemes, suitable for onboard applications have been identified. Another relevant property considered in this study is the predictability of the behavior of the relative motion during the reconfiguration, which concerns which values do the ROEs assume after each intermediate maneuver. Because many operational relevant features (e.g., delta-v minimization, safety, satisfaction of visibility constraints) are easily referable to well-defined geometries in the elements' space, a criterion to choose a reconfiguration strategy is provided by selecting those schemes whose maneuvers are conveniently located and directed to produce such aimed relative orbital elements' configurations.

Finally, mapping a reconfiguration in the relative orbital elements space revealed helpful to motivate the delta-v cost of each solution scheme, both regarding the value and the sources that contributed to that cost. The minimum realizable reconfiguration cost is expressed as a function of the total variation of the relative orbital elements in agreement with the widely known lower bound. Nevertheless, here a generalized expression that also includes changes in the mean relative longitude over a finite time span has been employed. Consequently, analytical and geometrical considerations allowed cross comparison of the costs achieved by each feasible reconfiguration strategy and relating them to the absolute minimum delta-v cost.

Possible further work comprises the extension of the analysis for the case when the chief satellite resides in an elliptic orbit. Other interesting applications consist of specific scenarios like tight proximity motions and satellites separation. In the former case, a maneuver scheme to achieve an aimed final condition shall comply with exclusion regions in the elements' space. In the latter case, maneuver schemes can be evaluated to efficiently reach safe zones of the elements' space.

Appendix: Remaining Equation Parameters

In the upcoming expressions, A, L, E, and F are the aimed ROE corrections according to Eq. (14). The coefficients that appear in J of Eq. (22) are the following functions of (ξ,E,F):

$$
\begin{aligned}
M_1 &= A_1E^2 + E_1F^2 + H_1EF,\\
N_1 &= B_1E^2 + F_1F^2 + I_1EF,\\
P_1 &= D_1E^2 + G_1F^2 + L_1EF\\
A_1 &= 128\sin\xi^2 + 36\xi^2(\cos^2\xi + 1) + 32(1-\cos\xi)^2\\
&\quad - 96\xi\sin\xi(1+\cos\xi)\\
B_1 &= -192\cos\xi(1-\cos\xi) + 72\xi^2(\sin^2\xi - 1)\\
&\quad + 192\xi\cos\xi\sin\xi\\
D_1 &= -96\sin\xi(1-\cos\xi) - 36\xi^2\sin\xi\cos\xi + 96\xi\sin^2\xi\\
E_1 &= 128(1-\cos\xi)^2 + 36\xi^2\sin^2\xi + 32\sin^2\xi\\
&\quad - 96\xi\sin\xi(1-\cos\xi)\\
F_1 &= 192\cos\xi(1-\cos\xi) + 72\xi^2(1-\sin^2\xi) - 192\xi\cos\xi\sin\xi\\
G_1 &= 96\sin\xi(1-\cos\xi) + 36\xi^2\sin\xi\cos\xi - 96\xi\sin^2\xi\\
H_1 &= 192\sin\xi(1-\cos\xi) - 192\xi\sin^2\xi + 72\xi^2\cos\xi\sin\xi\\
I_1 &= -384\sin\xi(1-\cos\xi) + 384\xi\sin^2\xi - 144\xi^2\cos\xi\sin\xi\\
L_1 &= 192\cos\xi(1-\cos\xi) - 192\xi\cos\xi\sin\xi + 72\xi^2\cos^2\xi
\end{aligned}
\tag{A1}
$$

The coefficients that appear in u_2 of Eq. (27) are functions of (u_0, u_F, A, L, E, F) according to

$$\tilde{D} = \cos u_0(3A \sin u_F - 3F) - 3E \sin u_F + \sin u_0(3E - 3A \cos u_F) + 3F \cos u_F$$

$$\tilde{K} = -(u_0(3F - 3A \sin u_F) + 3Au_F \sin u_F + 2L \sin u_F - 3Fu_F - 2L \sin u_0)/\tilde{D}$$

$$\tilde{P} = -(u_0(3A \cos u_F - 3E) - 3Au_F \cos u_F - 2L \cos u_F + 3Eu_F + 2L \cos u_0)/\tilde{D}$$

$$\tilde{Q} = -(\cos u_0(-3Au_F \sin u_F - 2L \sin u_F + 3Fu_F) + u_0(3E \sin u_F - 3F \cos u_F) + + \sin u_0(3Au_F \cos u_F + 2L \cos u_F - 3Eu_F))/\tilde{D} \quad \text{(A2)}$$

References

[1] D'Amico, S., and Montenbruck, O., "Proximity Operations of Formation Flying Spacecraft Using an Eccentricity/Inclination Vector Separation," *Journal of Guidance, Control, and Dynamics*, Vol. 29, No. 3, 2006, pp. 554–563. doi:10.2514/1.15114

[2] Clohessy, W. H., and Wiltshire, R. S., "Terminal Guidance System for Satellite Rendezvous," *Journal of the Aerospace Sciences*, Vol. 27, No. 9, 1960, pp. 653–658. doi:10.2514/8.8704

[3] Kechichian, J., and Kelly, T., "Analytical Solution of Perturbed Motion in Near-Circular Orbit Due to J2, J3 Earth Zonal Harmonics in Rotating and Inertial Cartesian Reference Frames," *AIAA 27th Aerospace Sciences Meeting*, AIAA Paper 1989-0352, Reno, Nevada, 1989.

[4] Carter, T. E., "State Transition Matrix for Terminal Rendezvous Studies: Brief Survey and New Example," *Journal of Guidance, Navigation, and Control*, Vol. 31, No. 1, 1998, pp. 148–155.

[5] Yamanaka, K., and Ankersen, F., "New State Transition Matrix for Relative Motion on an Arbitrary Elliptical Orbit," *Journal of Guidance, Control, and Dynamics*, Vol. 25, No. 1,2002, pp. 60–66. doi:10.2514/2.4875

[6] Lovell, T. A., and Tragesser, S. G., "Guidance for Relative Motion of Low Earth Orbit Spacecraft Based on Relative Orbit Elements," *AIAA Guidance, Navigation and Control Conference and Exhibit*, AIAA Paper 2004-4988, 2004.

[7] Ichimura, Y., and Ichikawa, A., "Optimal Impulsive Relative Orbit Transfer Along a Circular Orbit," *Journal of Guidance, Control, and Dynamics*, Vol. 31, No. 4, 2008, pp. 1014–1027.

[8] Schaub, H., "Relative Orbit Geometry Through Classical Orbit Element Differences," *Journal of Guidance, Control, and Dynamics*, Vol. 27, No. 5, 2004, pp. 839–848. doi:10.2514/1.12595

[9] Schaub, H., and Alfriend, K. T., "J2 Invariant Reference Orbits for Spacecraft Formations," *Celestial Mechanics and Dynamical Astronomy*, Vol. 79, No. 2, 2001, pp. 77–95.

[10] Schaub, H., "Incorporating Secular Drifts into the Orbit Element Difference Description of Relative Orbits," *13th AAS/AIAA Space Flight Mechanics Meeting*, American Astronautical Society Paper 2003-115, 2003.

[11] Harting, A., Rajasingh, C. K., Eckstein, M. C., Leibold, A. F., and Srinivasamurthy, K. N., "On the Collision Hazard of Colocated Geostationary Satellites," *AIAA/AAS Astrodynamics Conference*, AIAA Paper 1988-4239, 1988.

[12] Eckstein, M. C., Rajasingh, C. K., and Blumer, P., "Colocation Strategy and Collision Avoidance for the Geostationary Satellites at 19 Degrees West," *CNES International Symposium on SPACE DYNAMICS*, 1989.

[13] D'Amico, S., "Relative Orbital Elements as Integration Constants of Hill's Equations," DLR-GSOC TN-05-08, Oberpfaffenhofen, Germany, Dec. 2005.

[14] D'Amico, S., "Autonomous Formation Flying in Low Earth Orbit," Ph.D. Thesis, Technical Univ. of Delft, Delft, The Netherlands, March 2010.

[15] Gaias, G., Lavagna, M., Golikov, A., and Ovchinnikov, M. Y., "Formation Flying: Relative Orbits' Modelling and Control Through Eulerian Orbital Elements," *19th AAS/AIAA Space Flight Mechanics Meeting*, American Astronautical Society Paper 2009-186, 2009.

[16] Kasdin, N. J., Gurfil, P., and Kolemen, E., "Canonical Modeling of Relative Spacecraft Motion via Epicyclic Orbital Elements," *Celestial Mechanics and Dynamical Astronomy*, Vol. 92, No. 4, 2005, pp. 337–370.

[17] Alfriend, K., Vadali, S. R., Gurfil, P., How, J., and Breger, L., *Spacecraft Formation Flying: Dynamics, Control, and Navigation*, Butterworth-Heinemann, Oxford, U.K., 2010, pp. 147–149.

[18] Bodin, P., Noteborn, R., Larsson, R., Karlsson, T., D'Amico, S., Ardaens, J. S., Delpech, M., and Berges, J. C., "Prisma Formation Flying Demonstrator: Overview and Conclusions from the Nominal Mission," *35th Annual AAS Guidance and Control Conference*, American Astronautical Society Paper 2012-072, 2012.

[19] Rupp, T., Boge, T., Kiehling, R., and Sellmaier, F., "Flight Dynamics Challenges of the German On-Orbit Servicing Mission DEOS," *21st International Symposium on Space Flight Dynamics*, Toulouse, France, 2009.

[20] Tillerson, M., Inalhan, G., and How, J., "Co-Ordination and Control of Distributed Spacecraft Systems Using Convex Optimization Techniques," *International Journal of Robust Nonlinear Control*, Vol. 12, Nos. 2–3, 2002, pp. 207–242. doi:10.1002/rnc.683

[21] Tillerson, M., and How, J., "Advanced Guidance Algorithms for Spacecraft Formation-Keeping," *Proceedings of the American Control Conference*, Vol. 4, 2002, pp. 2830–2835. doi:10.1109/ACC.2002.1025218

[22] Larsson, R., Berge, S., Bodin, P., and Jönsson, U., "Fuel Efficient Relative Orbit Control Strategies for Formation Flying Rendezvous Within PRISMA," *Advances in the Astronautical Sciences*, Vol. 125, 2006, pp. 25–40.; also *29th Rocky Mountain Guidance and Control Conference*, AAS Paper 2006-025.

[23] Montenbruck, O., Kahle, R., D'Amico, S., and Ardaens, J.-S., "Navigation and Control of the TanDEM-X Formation," *Journal of Astronautical Sciences*, Vol. 56, No. 3, 2008, pp. 341–357.

[24] Vadali, S. R., Schaub, H., and Alfriend, K. T., "Initial Conditions and Fuel Optimal Control for Formation Flying of Satellites," *AIAA Guidance, Navigation, and Control Conference*, AIAA Paper 1999-4265, 1999.

[25] Schaub, H., and Alfriend, K. T., "Impulsive Feedback Control to Establish Specific Mean Orbit Elements of Spacecraft Formations," *Journal of Guidance, Control, and Dynamics*, Vol. 24, No. 4, 2001, pp. 739–745. doi:10.2514/2.4774

[26] Vaddi, S. S., Alfriend, K. T., Vadali, S. R., and Sengupta, P., "Formation Establishment and Reconfiguration Using Impulsive Control," *Journal of Guidance, Control, and Dynamics*, Vol. 28, No. 2, 2005, pp. 262–268. doi:10.2514/1.6687

[27] Jifuku, R., Ichikawa, A., and Bando, M., "Optimal Pulse Strategies for Relative Orbit Transfer Along a Circular Orbit," *Journal of Guidance, Control, and Dynamics*, Vol. 34, No. 5, 2011, pp. 1329–1341. doi:10.2514/1.51230

[28] D'Amico, S., Ardaens, J. S., and Larsson, R., "Spaceborne Autonomous Formation-Flying Experiment on the PRISMA Mission," *Journal of Guidance, Control, and Dynamics*, Vol. 35, No. 3, 2012, pp. 834–850. doi:10.2514/1.55638

[29] Ardaens, J. S., D'Amico, S., and Fischer, D., "Early Flight Results from the TanDEM-X Autonomous Formation Flying System," *4th International Conference on Spacecraft Formation Flying Missions*, 2011.

[30] Wang, J., Zhang, J., Cao, X., and Wang, F., "Optimal Satellite Formation Reconfiguration Strategy Based on Relative Orbital Elements," *Acta Astronautica*, Vol. 76, July–Aug. 2012, pp. 99–114. doi:10.1016/j.actaastro.2012.02.015

[31] Gaias, G., D'Amico, S., and Ardaens, J. S., "Generalized Multi-Impulsive Maneuvers for Optimum Spacecraft Rendezvous," *5th International Conference on Spacecraft Formation Flying Missions*, Munich, Germany, 2013.

[32] Eckstein, M. C., "Generalized Maneuver Planning for Station Keeping, Station Acquisition, Longitude Transfer and Reorbiting of Geostationary Satellites," DLR-GSOC TN-92-06, Oberpfaffenhofen, Germany, Nov. 1992.

[33] D'Amico, S., Ardaens, J. S., Gaias, G., Benninghoff, H., Schlepp, B., and Jørgensen, J. L., "Noncooperative Rendezvous Using Angles-Only Optical Navigation: System Design and Flight Results," *Journal of Guidance, Control, and Dynamics*, Vol. 36, No. 6, 2013, pp. 1576–1595. doi:10.2514/1.59236